Yields of fission products produced by thermal-neutron fission of ^{245}Cm

J. K. Dickens and J. W. McConnell
Oak Ridge National Laboratory, Oak Ridge, Tennessee 37830
(Received 14 July 1980)

Absolute yields have been determined for 105 gamma rays emitted in the decay of 95 fission products representing 54 mass chains created during thermal-neutron fission of ^{245}Cm. These results include 17 mass chains for which no prior yield data exist. Using a Ge(Li) detector, spectra were obtained of gamma rays between 30 sec and 0.3 yr after very short irradiations of thermal neutrons on a 1 μg sample of ^{245}Cm. On the basis of measured gamma-ray yields and known nuclear data, total chain mass yields and relative uncertainties were obtained for 51 masses between 84 and 156. The absolute overall normalization uncertainty is $<8\%$. The measured A-chain cumulative yields make up 81% of the total light mass ($A \leq 121$) yield and 92% of the total heavy mass yield. The results are compared with fission-product yields previously measured with generally good agreement. The mass-yield data have been compared with those for thermal-neutron fission of ^{239}Pu and for ^{252}Cf(s.f.); the influences of the closed shells $Z = 50$, $N = 82$ are not as marked as for thermal-neutron fission of ^{239}Pu but much more apparent than for ^{252}Cf(s.f.). Information on the charge distribution along several isobaric mass chains was obtained by determining fractional yields for 12 fission products. The charge distribution width parameter, based upon data for the heavy masses, $A = 128$ to 140, is independent of mass to within the uncertainties of the measurements. Gamma-ray assignments were made for decay of short-lived fission products for which absolute gamma-ray transition probabilities are either not known or in doubt. Absolute gamma-ray transition probabilities were determined as $(51 \pm 8)\%$ for the 374-keV gamma ray from decay of ^{110}Rh, $(35 \pm 7)\%$ for the 1096-keV gamma ray from decay of ^{133}Sb, and $(21.2 \pm 1.2)\%$ for the 255-keV gamma ray from decay of ^{142}Ba.

[RADIOACTIVITY, FISSION ^{245}Cm(n,f) E_n= thermal; measured $\sigma(E_\gamma, T_{1/2})$; deduced mass, charge yields.]

INTRODUCTION

Although published data on mass and charge distributions of the fission products following prompt neutron emission in thermal-neutron induced and spontaneous fission cover fissioning systems between ^{228}Th and ^{258}Fm, most of the data are concentrated in the ^{234}U (i.e., $n_{\text{thermal}}+^{233}$U), ^{236}U, ^{240}U, and ^{252}Cf systems. Even for these systems the data are not complete, and evaluators[1,2] must rely to some extent on semiempirical methods to provide complete evaluations of mass chain yields. The mass distributions of all but the heaviest fissioning systems are predominantely asymmetric. The major variations observed in mass distributions as a function of increasing mass of the fissioning system are a shift in the peak of the light mass distribution and an overall broadening of the distribution of fission products created in both the light and heavy mass groups. For the lighter fissioning systems, particularly for ^{234}U, ^{236}U, and ^{240}Pu, yields for the fission product masses 125 to 133 are very similar, increasing from about 0.1% for mass 125 to about 6% for mass 133. It has been suggested[3] that the double shell closure $Z = 50$ (Sn) and $N = 82$ has a marked influence on the mass yields in low-energy fission for these systems. However the heavy fission-product mass distribution[4] for ^{252}Cf(s.f.) has definitely shifted toward heavier fission-product production. It is of interest to determine the character of the transitions in fission product yields from systems between the ^{240}Pu fissioning system and the ^{252}Cf system; the ^{246}Cm system, from thermal-neutron fission of ^{245}Cm, is perhaps the most amenable for study.

There is another, rather pragmatic, reason for determining fission-product yields for thermal-neutron fission of ^{245}Cm. About 90% of the fission products created during ^{252}Cf production at Savannah River arise from ^{245}Cm fission,[5] and a substantial percentage of fission products created during transplutonium isotope production at the High Flux Isotope Reactor at ORNL is due to ^{245}Cm fission by thermal neutrons. For these, and other reasons, there have been three experiments[5-7] performed during the last 15 years designed to measure mass yields for thermal-neutron fission of ^{245}Cm over the whole mass distribution; in addition, a few experiments have been reported[8-11] devoted to measurements of a few fission products in order to determine charge distributions. The major difficulty encountered in all of these experiments has been the inability to acquire enough ^{245}Cm material to perform the radiochemical separations generally used in fission-product yield measurements. In all of the experiments quoted[5-11] the sample amounts of ^{245}Cm used were ≈ 1 μg. In the first experiment reported, von Gunten *et al.*[6] did utilize radiochemical separations so that beta-

ray counting methods could be used. Subsequent experiments have depended solely on gamma-ray counting without chemical separations. All of these experiments determined *ratios* of yields with respect to $n_{thermal}+^{235}U$ fission-product yields. Thus, uncertainties in detection efficiencies, detector responses, and beta- or gamma-ray decay probabilities were exchanged for uncertainties in ^{235}U fission-product yields, uncertainties in sample variables of *two* samples, and for uncertainties associated with large differences in fission-product yields for the ^{236}U and ^{246}Cm systems in the mass region 109 to 115. Measurements were limited in all three experiments to the longer-lived fission products (half-life >30 min). Consequently, less than half of the total mass yield has been determined empirically. Overall mass yield curves were determined for all three principal experiments by assuming that measured yield data could be reflected about the symmetric fission mass (~ mass 121), and at least for two of the three experiments the resulting total mass distribution was normalized to 200%. It may be expected that this procedure will be approximate, since based upon measured mass distributions for $n_{thermal}+^{239}Pu$ and ^{252}Cf (s.f.) light mass fission-product distribution for $n_{thermal}+^{245}Cm$ may be only an approximate reflection of the heavy mass fission-product distribution. Evidently, yields for fission products having short half-lives are needed to fill out the mass distributions in more detail.

Recently, we measured[12] fission-product yields due to thermal-neutron fission of ^{239}Pu using gamma-ray counting of unseparated fission products. Since only one sample was used and there were no chemical separations, gamma-ray counting began when the sample radioactivity had decreased to a satisfactory level, which in that experiment was ~20 min after a 100 sec irradiation of a 1 μg ^{239}Pu sample. We learned that observed gamma rays could be reliably assigned to decay of specific fission products by matching E_γ and measured lifetimes, and consequently were able to obtain yields for fission products in that experiment having half-lives as short as 10 min. The number of fissions induced in the ^{239}Pu sample was determined by a "K-factor" method developed previously.[13] About 65% of the total mass yield was deduced from these ^{239}Pu fission-product measurements.[12]

Because of the need for definitive fission-product yield data for the ORNL transplutonium isotope production program, a similar experiment was performed for a 1 μg sample of ^{245}Cm, with two major differences. The first was that several irradiation periods, tailored to allow initial gamma-ray measurements to begin <1 min after a very short irradiation, were used. In addition, the total measurement period was extended to ~0.3 yr to obtain data on longer-lived fission products. The second difference was that there was not enough ^{245}Cm available to develop a "K-factor" method of determining the number of fissions in the ^{245}Cm sample as had been done for the ^{239}Pu measurement. Hence, we relied on a measurement of the thermal neutron flux and thermal-to-epithermal ratio at the position of irradiation and a measure of the sample size to determine the number of fissions. The determination of the number of fissions in this manner was later verified by determining the total mass yield based upon our measurements and comparing to the expected 200%; it should be noted that the overall normalization of the present data was *not* adjusted to agree with the expected 200% total. Yields were deduced for ~90 fission products, some having half-lives <1 min.

Much of the uncertainty associated with the present fission-product yield determinations, particularly for the short-lived isotopes, is associated with uncertainties in nuclear data, especially gamma-ray decay probabilities (i.e., branching ratios). In fact, yields were measured for gamma rays which could be assigned to fission products for which absolute branching ratios have not yet been reported. Improved nuclear data will result in a more complete set of yield data than can be presented at the present time. With current knowledge of relevant nuclear data, the present experiment identifies ~86% of the total mass yield. The missing ~14% has been determined by interpolation rather than by using the reflection method. In addition, the present data provide a sufficient amount of information about charge distributions so that, at least for the heavy fission products, parameters needed for estimation of yields of very short-lived fission products can be obtained from the data.

EXPERIMENTAL DATA ACQUISITION

The ^{245}Cm sample for these studies was obtained by chemically separating the Cm from a sample of ^{249}Cf which was several months old. Alpha-particle measurements were made on a small aliquot of this material, and these indicated ~0.2% by mass of ^{249}Cf in the sample. The α activity measured for the total material milked from the ^{249}Cf sample (15.2 ± 0.4) kBq of which (14.1 ± 0.4) kBq was due to decay of ^{245}Cm. One-half of the total ^{245}Cm, corresponding to ~1 μg of Cm enriched in the ^{245}Cm isotope to >99%, was allocated to the sample we used. In addition, preliminary gamma-ray measurements indicated no evidence for gamma rays emanating from fission products in the sample.

For our experiment the sample, in the chemical

form of curium nitrate, was deposited and dried in a small polyethylene container of wall thickness ~0.5 kg/m^2 and covered with a lid of similar thickness. This container was then placed inside a polyethylene capsule designed for pneumatic transfer to and from an irradiation position at the Oak Ridge Research Reactor (ORR). Details of the gamma-ray container and capsule have been reported.[14] The neutron flux at the irradiation position was ~4.5×10^{13} n/cm^2 s, and the ratio of thermal neutrons to resonance energy neutrons was ~30:1, measured using gold and manganese foils, and calculated assuming an E^{-1} epithermal flux.

Three irradiation periods, 4 s, 40 s, and 6 min, were used. The sample was rapidly recovered following irradiation so that measurements in a fixed counting geometry could begin within 30 s following the end of irradiation. The timing parameters were selected to facilitate the interpretation of the results of fission products having "short" (to 10 min), "intermediate" (to 100 h), and "long" (to 1 yr) half-lives. Following the 4-s irradiation, data were obtained between 30 s and 45 min after the irradiation in 20 separate 4096-channel pulse-height spectra. Following the 40-s irradiation, data were obtained between 25 min and 21 d after the irradiation, and following the 6-min irradiation data were obtained between 1 d and 0.3 yr after the irradiation. Altogether ~115 4096-channel pulse-height spectra were obtained and analyzed.

Gamma-ray measurements were made through the ~2 kg/m^2 end of the capsule using two detector systems: (1) a 45-cm^3 Ge(Li) at the ORR close to the pneumatic-tube facility in a rather high-background area was used to obtain data following the 4-s irradiation; and (2) a well shielded 90-cm^3 Ge(Li) detector in a low-background area was used to obtain data following the 40-s and 6-min irradiations. For cooling times <3 h a 9.7 kg/m^2 carbon plate was placed close to the sample to absorb beta radiation emanating from the sample. Corrections for reduction in detection efficiency caused by this absorber were obtained using standard tables[15] of gamma ray attenuation. Amplifier time constants of 3 μs were used for good energy resolution; corrections for random summing were determined empirically[16] and were equivalent to a "dead-time" constant of ~7 μs. The sample-to-detector distances were 0.3 m for measurements using the 45-cm^3 detector and 0.2 m for measurements using the 90-cm^3 detector. These distances were chosen to minimize true coincidence effects in the detector and dead-time losses, as well as to minimize the contribution to the overall uncertainty due to any uncertainty in measurements of the source-to-detector distances. A spectrum obtained using the 45-cm^3 detector is given in Fig. 1, and a spectrum obtained with the 90-cm^3 detector is given in Figs. 2(a) and 2(b). In the latter case essentially all of the sources of the observed gamma rays have been identified; one may choose gamma rays to analyze which are sufficiently isolated from other gamma-ray data. The data shown in Fig. 1 are considerably more complex.

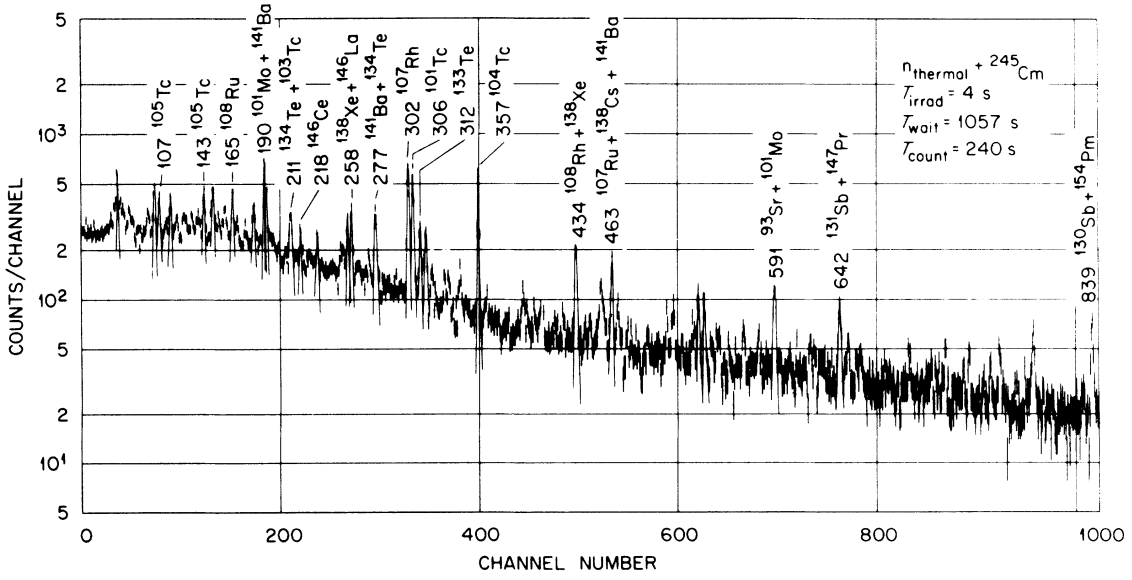

FIG. 1. Pulse-height spectrum of gamma rays following a 4-s irradiation of a ^{245}Cm sample by thermal neutrons. Symbols indicate gamma-ray energy (in keV) and isotopic assignment.

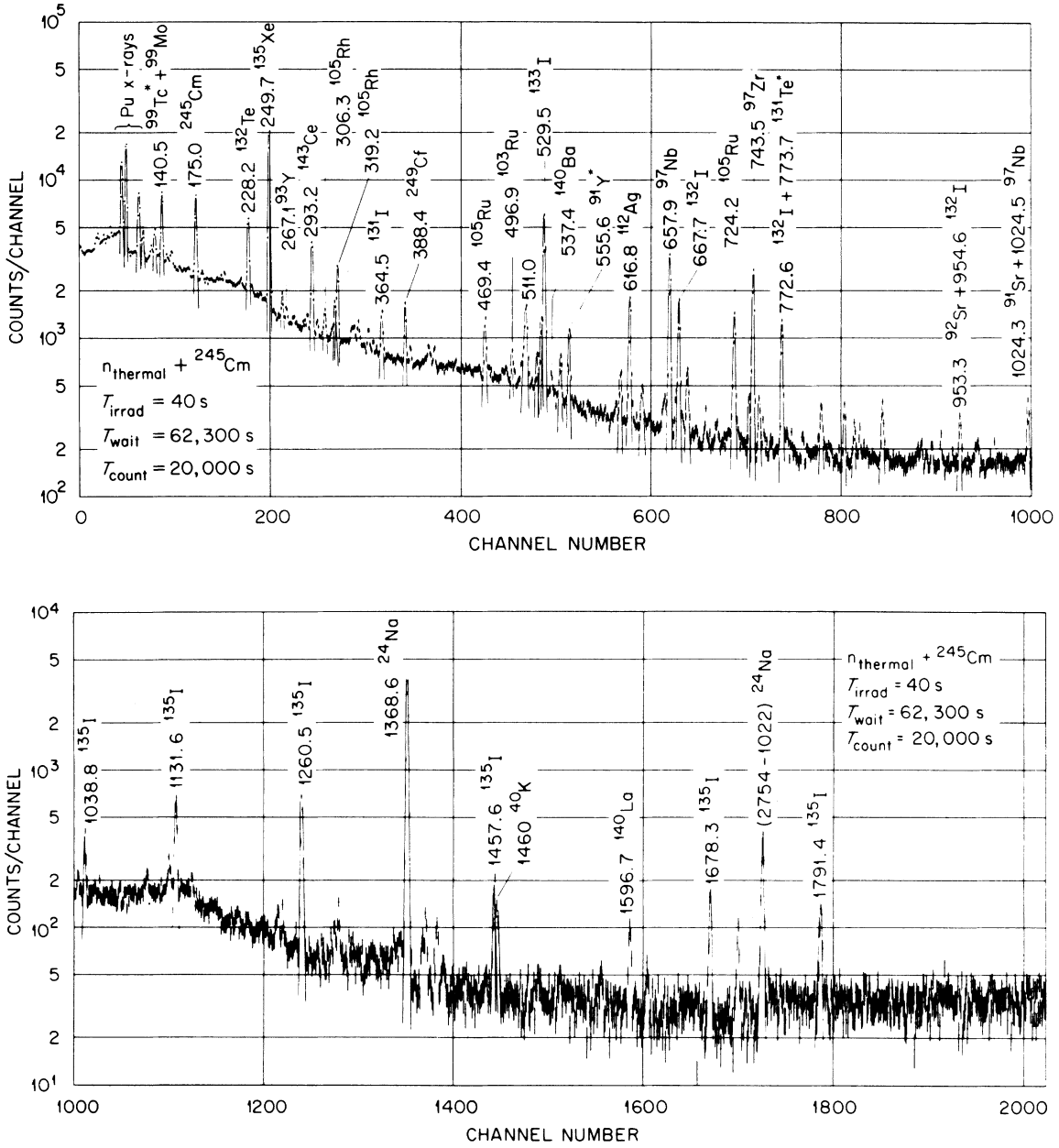

FIG. 2. (a) Pulse-height spectrum of gamma rays following a 40-s irradiation of a ^{245}Cm sample by thermal neutrons. Nearly all peaks are identified with known fission product decay. (b) High-energy portion of the spectrum shown in (a).

DATA REDUCTION

To determine fission product yields (C), both the efficiency $\epsilon(E_\gamma)$ and the fraction of the decay of the fission product giving the desired gamma ray (B) are required. For the 90-cm^3 detector, the detector efficiency $\epsilon(E_\gamma)$ versus E_γ was determined for 60 keV $\leq E_\gamma \leq$ 1836 keV using well calibrated commercially obtained radioactive sources; the calibration has been discussed in detail in a previous report.[14] For a source-to-detector distance of 200 mm, the uncertainty in $\epsilon(E_\gamma)$ is <2% (one standard deviation). For the 45-cm^3 detector the efficiency $\epsilon(E_\gamma)$ versus E_γ was supplied by personnel responsible[17] for this detector with an estimated uncertainty of ~2%; during the present experiment the given $\epsilon(E_\gamma)$ were checked and found to reproduce to within ~2% expected gamma-ray intensities for E_γ>180 keV using a calibrated source of ^{226}Ra. The pulse-height data were reduced using a com-

puter routine[18] written for the ORNL decay heat program. For single peaks, the peak areas were extracted using the computer routine; doublets were also usually adequately analyzed for individual peak areas by the code. Multiplet (more than two) peaks are passed over by the code; some of these were analyzed manually to obtain information on an important gamma ray.

Energies E_γ were assigned to the peaks that had been analyzed, and these were used to obtain the efficiency $\epsilon(E_\gamma)$. Then, the gamma-ray intensities were determined as a function of time following irradiation. Assignment to a particular fission product was based upon matching the experimental gamma-ray energy with the known fission-product gamma-ray energy to ±1 keV and in addition matching the fission-product half-life with the experimental "half-life" to within the uncertainty associated with the measurement. General relationships for independent yields and half-lives for all nuclides in a given mass chain are well known.[19-22] For the present data, it was sufficient to include only one parent and one daughter decay, since most of the precursor nuclides have very short lifetimes and had decayed completely by the initiation of the first gamma-ray counting period. Also, the irradiation periods were much shorter than the cooling periods and so were approximated as instantaneous irradiations. Thus, the yield (Y) in a particular measurement of a given gamma ray due to decay of a fission product and of its parent is given by

$$[(Y/\epsilon)/B]_d = n_f C_p^c \left\{ \frac{\lambda_p}{\lambda_p - \lambda_d} \exp(-\lambda_d T)[1 - \exp(-\lambda_d t_c)] - \frac{\lambda_d}{\lambda_p - \lambda_d} \exp(-\lambda_p T)[1 - \exp(-\lambda_p t_c)] \right\} + n_f C_d^i \exp(-\lambda_d T)[1 - \exp(-\lambda_d t_c)], \quad (1)$$

where λ is the decay constant for a particular nuclide, T and t_c are, respectively, the cooling and counting times, the subscript d is for the (daughter) fission product being analyzed, and the subscript p is for the parent. Here, C^i is the independent yield, and C^c is the cumulative fission yield.

For much of the data, the half-life of the parent is sufficiently different from that of the daughter that the analysis of the data could be performed in the limiting cases. For $\lambda_p \ll \lambda_d$

$$[(Y/\epsilon)/B]_d \to n_f C_p^c \frac{\lambda_d}{\lambda_d - \lambda_p} e^{-\lambda_p T}(1 - e^{-\lambda_p t_c}), \quad (2)$$

and it is the cumulative fission yield of the parent which is obtained. For $\lambda_p \gg \lambda_d$

$$[(Y/\epsilon)/B]_d \to n_f \left(C_d^i + C_p^c \frac{\lambda_p}{\lambda_p - \lambda_d} \right) e^{-\lambda_d T}(1 - e^{-\lambda_d t_c}), \quad (3)$$

and the cumulative fission yield of the daughter is obtained from

$$C_d^c = C_d^i + C_p^c. \quad (4)$$

Details of least-squares mathematics required for the solution of Eq. (2) or (3) have been reported.[23] The steps involved were (a) to obtain the efficiency-corrected counting rate Y/ϵ at the beginning of each counting period, and (b) to obtain the $T=0$ counting rate intercept Y_0/ϵ and its uncertainty by the least-squares analysis. The cumulative yield was then obtained from the applicable Eq. (2), or Eq. (3) plus Eq. (4). The uncertainty ΔC was obtained by appropriately combining uncertainties $\Delta(Y_0/\epsilon)$, Δn_f, $\Delta\lambda$, and ΔB.

Several spectra had high count rates, requiring corrections due to random summing. As a check on this correction, as well as a check on the live-time clock on the analyzer, data for 37-min ^{38}Cl and for 15-h ^{24}Na were analyzed. These isotopes were created during the irradiation from NaCl contaminant. The counting rates for gamma rays from these isotopes were large enough to obtain a good analysis of counting losses, but not large enough to interfere with data reduction of the fission products of interest. This check verified that the corrections which were made were satisfactory to within the 20% uncertainty (i.e., 20% of the dead-time correction used) assigned to the correction.

Data for some of the peaks observed represented nearly degenerate gamma rays from decay of two independent nuclides; an example is $E_\gamma = 590.6$ keV observed as a single, slightly broadened peak. This peak is due to two transitions, viz., $E_\gamma = 590.3$ keV from decay of 7.4-min ^{93}Sr and $E_\gamma = 590.9$ keV from decay of 14.6-min ^{101}Mo. When the half-lives were sufficiently different, such data were analyzed first to obtain results for the longer-lived nuclide; then following an appropriate subtraction of the component due to the longer-lived nuclide, the data were analyzed a second time to obtain results for the shorter-lived nuclide. For $E_\gamma = 590.6$ keV, however, the data were analyzed using a least-squares method to separate the two contributions. The latter method worked well on all cases tried except those for $E_\gamma = 697$ and 974 keV; these gamma rays occur in the decay of ^{132}Sb (168 s) and ^{132}Sb* (252 s), and since a reasonable separation of the individual contributions could not be obtained, the results for these two gamma rays represent the sum of ^{132}Sb and ^{132}Sb* contributions.

Data for twelve gamma rays representing ten parent-daughter contributions were analyzed using Eq. (1) to obtain the fractional contribution to the observed data from both the decay of the daughter and the parent. An example of this type of analysis is shown in Fig. 3 for ^{134}Te → ^{134}I → ^{134}Xe, E_γ

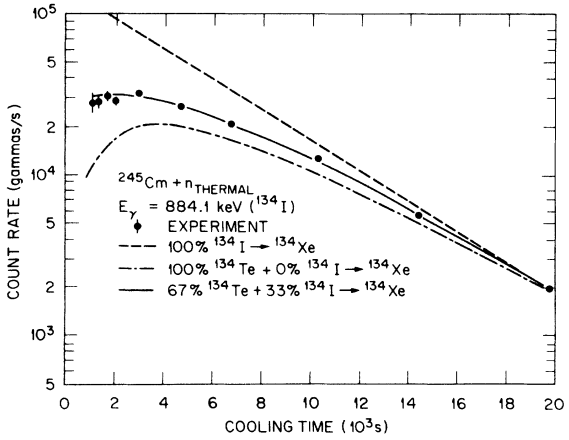

FIG. 3. Analysis of data obtained for $E_\gamma = 884.1$ keV assigned to decay of ^{134}I. A least-squares analysis of the these data was determined the best fit to the data as shown by the solid line. The dashed and dot-dashed lines indicate the time dependence of the decay of this gamma ray under different initial concentrations of ^{134}Te and ^{134}I.

= 884 keV due to decay of ^{134}I. Results of these analyses are given in Table I. A complete discussion of the least-squares mathematics is given in subsection B of the Discussion.

For the shortest-lived and longest-lived nuclides studied, data were available in only a few spectra. For these cases an estimate for Y_0/ϵ was obtained from each spectrum; that is,

$$(Y_0/\epsilon)_i = (Y_i[T_i, t_{ci}]/\epsilon)\exp(\lambda T_i), \quad i = 1, \ldots, n \quad (5)$$

was determined for each of n spectra having appropriate data. Then the "best" value of Y_0/ϵ and its uncertainty was obtained from the set of $(Y_0/\epsilon)_i$ and associated uncertainties.

The number of fissions created in the 6-min irradiation was determined from the knowledge of the mass, neutron flux, irradiation time, and thermal and resonance-integral fission cross sections (2030 and 750 b, respectively[24]), and was 9.2×10^{10} fissions. Since the neutron flux impinging on the sample included nonthermal neutrons, ~1% of the fissions in the ^{245}Cm were due to epithermal neutron interactions. It was assumed that the mass and charge distributions due to this nonthermal neutron fission in the sample were the same as for thermal-neutron fission for the fission-product yields deduced from the data. The uncertainty in n_f was determined by quadratically combining a 3% uncertainty in mass, 5% uncertainty in neutron flux, and 5% uncertainties in the fission cross sections[25] for a total uncertainty of ~7.7%. Data for the 40-s irradiation were normalized to those for the 6-min irradiation with an added normalization uncertainty of ~1%, and data for the 4-s irradiation were normalized to those for the 40-s irradiation with an added uncertainty of 2%. These latter two normalization uncertainties are included in the tabulated results; the overall uncertainty of ~7.7% is not. As discussed later, the measured yields were summed and compared with the expected 100% for light masses and 100% for heavy masses, and the agreement is sufficient to warrant an overall normalization uncertainty <7.7%.

The data reduction gives values of yield/fission for selected gamma rays, the selection being based upon identification with specific products. These are tabulated in Table II, along with relative uncertainties. There were many gamma rays observed for which yield/fission results were not obtained, even though the gamma ray could have been ascribed to decay of a specific fission product. We were satisfied with analyzing only one or two gamma rays associated with decay of a given fission product, usually but not always the gamma ray with the largest branching ratio (B). We attempted to obtain information for at least one fis-

TABLE I. Partial yields from thermal neutron fission of ^{245}Cm.

Mass	E_γ (keV)	Parent ($T_{1/2}$)	Daughter ($T_{1/2}$)	$C_d/(C_p + C_d)$ (%)
95	765.8	Zr(65 d)	Nb(35 d)	1.2 ± 0.5
109	326.6	Ru(34 s)	Rh(80 s)	21 ±12
112	617.4	Pd(21 h)	Ag(3.1 h)	2.4 ± 1.5
130	839.4	Sn(222 s)	Sb(390 s)	48 ±24
132	667.7	Te(76 h)	I(2.3 h)	5.20± 0.44
134	884.1	Te(41.8 min)	I(52.6 min)	32.7 ± 1.8
134	1072.6	Te(41.8 min)	I(52.6 min)	31.4 ± 4.9
135	526.6	I(6.61 h)	Xe*(15.6 min)	40 ± 4
135	249.8	I(6.61 h)	Xe(9.08 h)	14.6 ± 0.6
138	1435.9	Xe(14.2 min)	Cs(32.2 min)	23.1 ± 4.8
140	487.0	Ba(307 h)	La(40.2 h)	0.50± 0.30
140	1596.6	Ba(307 h)	La(40.2 h)	0.64± 0.23

TABLE II. Intensities of gamma rays associated with decay of fission products created by thermal-neutron fission of ^{245}Cm and deduced fission-products yields.

E_γ (keV) [a]	Yield per 100 fissions	Assigned fission product	Gamma-ray branching ratio (%) [b]	$T_{1/2}$ (s)	$T_{1/2}$ (parent) (s)	Cumulative fission product yield (%)
91.1	0.73 ±0.03	^{147}Nd	27.9 ±0.5	9.56 *E*5	780	2.63 ±0.10
116.7	0.43 ±0.03	^{151}Nd	46.8 ±3.6	746	4	0.92 ±0.10
120.9, 121.8	0.29 ±0.07	^{90}Kr	35.5 ±3.0	32.3	2.0	0.83 ±0.21
121.8	0.23 ±0.11	^{152}Pm	16 ±2	252	702	1.4 ±0.7
127.3	0.10 ±0.08	^{153}Pm	15 ±3 [c]	324	(short)	0.67 ±0.54
137.72	2.63 ±0.17	^{99}Nb	90 ±2	15	3	2.34 ±0.18
140.51	3.69 ±0.12	^{99}Mo	90.7 ±0.6	2.38 *E*5	15	4.10 ±0.13
143.26	0.98 ±0.05	^{105}Tc	(11 ±1) [d]	456	36	(8.9 ±0.9) [d]
145.4	2.60 ±0.07	^{141}Ce	48.2 ±0.3 [e]	2.81 *E*6	14 040	5.38 ±0.16
165.0	1.54 ±0.10	^{108}Ru	28 ±7	270	5	5.5 ±1.4
165.84	1.63 ±0.06	^{139}Ba	22 ±4	4962	570	6.6 ±1.2
206.2 [f]	0.91 ±0.09	^{109}Ru	unknown	34.5	1.4	
211.3	0.51 ±0.03	^{149}Nd	25.9 ±1.3 [g]	6228	138	1.94 ±0.15
218.25	0.54 ±0.06	^{146}Ce	20.5 ±3.2	834	11	2.68 ±0.49
218.75	2.39 ±0.18	^{139}Xe	50 ±6	39.7	2.3	4.8 ±0.7
228.33	3.54 ±0.10	^{132}Te	88.2 ±0.2	2.75 *E*5	168, 252	4.01 ±0.11
249.8	5.45 ±0.12	^{135}Xe	90 ±3	32 760	23 800	6.06 ±0.24
255.30	0.85 ±0.05	^{142}Ba	20.0 ±1.8	636	1.7	4.24 ±0.46
258.41	1.52 ±0.09	^{138}Xe	31.5 ±1.3	850	6.5	4.83 ±0.32
266.9	0.131 ±0.010	^{93}Y	6.8 ±0.4	36 900	446	1.93 ±0.19
270.10	2.98 ±0.25	^{106}Tc	56 ±3 [t]	36	9.5	5.32 ±0.53
271.9	0.89 ±0.07	^{134}I*	79 ±3	230	(short)	1.12 ±0.10
275.3 [f]	2.8 ±1.5	^{111}Rh	unknown	11	1.6	
291.8 [h]	1.00 ±0.25	^{148}Ce	unknown	48	1.3	
293.28	1.93 ±0.06	^{143}Ce	43.4 ±2.0	1.19 *E*5	840	4.40 ±0.24
298.4	0.18 ±0.02	^{113}Ag	9 ±1 [i]	19 330	90	(2.0 ±0.3) [d]
301.70	0.84 ±0.38	^{148}Pr	unknown [j]	140	48	
302.86	3.61 ±0.20	^{107}Rh	65.9 ±4.6	1302	252	5.5 ±0.5
316.76	1.52 ±0.09	^{146}Ce	52.5 ±5.7	834	11	2.88 ±0.36
318.9	1.32 ±0.07	^{105}Rh	19.2 ±0.2	1.28 *E*5	15 984	6.03 ±0.32
326.45	2.31 ±0.19	^{109}Rh	62 ±7 [k]	80	34	3.73 ±0.52
336.2	0.285 ±0.013	^{115}In*	45.9 ±0.1	16 160	1.93 *E*5	0.57 ±0.03 [r]
340.1	0.264 ±0.017	^{151}Pm	22.3 ±0.5	1.03 *E*5	746	1.18 ±0.08
342.1	0.250 ±0.059	^{111}Ag	6.7 ±0.5 [l]	6.46 *E*5	13 290, 19 840	3.7 ±0.9
343.67	0.569 ±0.042	^{141}Ba	14.2 ±1.2	1096	25	4.01 ±0.45
346.38	1.14 ±0.14	^{103}Tc	16.3 ±3.0 [m]	50	67	7.0 ±1.6
357.95	5.94 ±0.21	^{104}Tc	89 ±5	1086	60	6.67 ±0.42
364.5	2.59 ±0.07	^{131}I	82.5 ±0.4	6.94 *E*5	1500, 1.08 *E*5	2.82 ±0.08
373.8	2.0 ±0.2	^{110}Rh	unknown	3	16	
381.35	1.60 ±0.13	^{136}I*	99.8 ±5.5	44.8	17.5	1.53 ±0.14
397.44	3.94 ±0.18	^{144}La	90 ±5 [n]	42	1	4.31 ±0.31
402.59	0.251 ±0.018	^{87}Kr	49.5 ±1.6	4579	56	0.50 ±0.04
407.58	0.835 ±0.054	^{133}Te	32.7 ±0.4	745	150, (3324)	2.00 ±0.16
453.89	1.28 ±0.09	^{146}Pr	48 ±3	1440	834	2.66 ±0.25
455.51	1.52 ±0.24	^{137}Xe	31 ±3	229	25	4.9 ±0.9
469.4	1.23 ±0.30	^{105}Ru	18.0 ±0.7	15 984	456	6.64 ±0.31
475.22	0.362 ±0.042	^{102}Tc	6.25 ±1.0 [o]	5.3	660	5.8 ±1.2 [r]
482.15	0.276 ±0.018	^{128}Sn	62.3 ±6.2	3546	≤12	0.44 ±0.05
487.0	2.44 ±0.07	^{140}La	43.0 ±1.4	1.15 *E*5	1.11 *E*6	5.68 ±0.25

TABLE II. *(Continued)*

E_γ (keV) [a]	Yield per 100 fissions	Assigned fission product	Gamma-ray branching ratio (%) [b]	$T_{1/2}$ (s)	$T_{1/2}$ (parent) (s)	Cumulative fission product yield (%)
497.1	5.62 ± 0.17	^{103}Ru	90.9 ± 0.7	3.40 *E*6	50	6.18 ± 0.19
526.6	1.12 ± 0.07	^{135}Xe*	81 ± 1	939	23 800	1.38 ± 0.07
529.97	4.83 ± 0.15	^{133}I	87.3 ± 0.2	74 880	{745 / 3324}	5.39 ± 0.16
531.0	0.31 ± 0.09	^{147}Nd	13.1 ± 0.8	9.56 *E*5	780	2.33 ± 0.17
537.60	1.31 ± 0.04	^{140}Ba	24.4 ± 0.2	1.11 *E*6	65.5	5.39 ± 0.16
555.6	0.714 ± 0.025	^{91}Y	95.1 ± 0.1	3000	34 680	0.686 ± 0.023
558.0	0.215 ± 0.060	^{114}Ag	12 ± 3 [p]	4.5	144	1.8 ± 0.7 [r]
566.08	0.738 ± 0.033	^{134}Te	18.8 ± 1.0	2508	11	3.92 ± 0.27
590.24	0.68 ± 0.13	^{93}Sr	73 ± 8	446	6	0.93 ± 0.20
590.88	1.11 ± 0.09	^{101}Mo	19.4 ± 1.0	887	7	5.70 ± 0.52
600.5	0.09 ± 0.04	^{137}I	6.8 ± 2.3	24.5	4	1.2 ± 0.7
602.35	2.61 ± 0.15	^{140}Cs	72 ± 3	65.5	13.6	(3.47 ± 0.25) [d]
617.4	1.44 ± 0.05	^{112}Ag	42 ± 5	11 300	75 600	3.42 ± 0.43
622.2	0.558 ± 0.022	^{106}Rh	9.8 ± 0.5	30	3.17 *E*7	5.7 ± 0.4 [r]
641.29	2.73 ± 0.10	^{142}La	52.5 ± 2.5	5580	636	4.67 ± 0.28
657.9	3.16 ± 0.09	^{97}Nb	98.34 ± 0.11	432	60 840	2.99 ± 0.09 [r]
667.76	4.11 ± 0.13	^{132}I	98.7 ± 0.1	8222	2.75 *E*5	4.16 ± 0.13
685.7	0.160 ± 0.012	^{127}Sb	36.6 ± 0.5	3.33 *E*5	7560	0.426 ± 0.034
697.05	1.79 ± 0.10	{^{132}Sb / ^{132}Sb*}	{86 ± 4 / 99.5 ± 0.2}	{168 / 252}	40	1.83 ± 0.15
724.30	3.23 ± 0.10	^{105}Ru	48 ± 1	15 984	456	6.53 ± 0.25
724.3	2.37 ± 0.12	^{145}Ce	68 ± 5	180	30	3.04 ± 0.27
743.4	2.64 ± 0.10	^{97}Zr	97.96 ± 0.06	60 840	4	2.69 ± 0.20
754.0	0.590 ± 0.043	^{128}Sb*	99.75 ± 0.15	600	3546	0.59 ± 0.04
754.0	0.086 ± 0.009	^{128}Sb	99.75 ± 0.15	32 580	(short)	0.09 ± 0.01
756.7	1.28 ± 0.11	^{95}Zr	54.6 ± 0.5	5.53 *E*6	618	2.35 ± 0.19
765.8	2.27 ± 0.07	^{95}Nb	99.82 ± 0.01	3.02 *E*6	5.53 *E*6	2.28 ± 0.07
812.8	0.478 ± 0.019	^{129}Sb	45.0 ± 4.5	15 550	{132 / 450}	1.06 ± 0.12
839.52	0.799 ± 0.042	^{130}Sb	99.8 ± 0.1	2400	102	0.799 ± 0.042
839.52	0.94 ± 0.10	^{130}Sb*	99.8 ± 0.1	390	222	0.94 ± 0.10
852.2	0.199 ± 0.013	^{131}Te*	21.3 ± 0.9	1.08 *E*5	1382	0.93 ± 0.07
884.31	3.90 ± 0.14	^{134}I	65.3 ± 1.0	3156	2508	5.97 ± 0.23
912.7	1.80 ± 0.07	^{133}Te*	62.8 ± 2.6	3324	150	2.72 ± 0.16
918.74	0.946 ± 0.037	^{94}Y	56 ± 3	1122	75	1.61 ± 0.11
934.4	1.00 ± 0.05	^{131}Sb	44.0 ± 4.4	1382	63	2.24 ± 0.24
973.9	1.97 ± 0.12	{^{132}Sb / ^{132}Sb*}	{99.9 ± 0.1 / 99.9 ± 0.1}	{168 / 252}	40	1.94 ± 0.12
1024.3	0.390 ± 0.017	^{91}Sr	33.5 ± 0.7	34 680	59	1.18 ± 0.06
1031.9	0.591 ± 0.040	^{89}Rb	58 ± 5	909	190	0.82 ± 0.09
1048.1	0.100 ± 0.004	^{136}Cs	79.8 ± 0.9	1.13 *E*6	shielded	0.125 ± 0.006 [s]
1072.5	0.812 ± 0.055	^{134}I	15.3 ± 0.8	3156	2508	5.31 ± 0.45
1096.2	0.40 ± 0.06	^{133}Sb	unknown	150	2	
1114.3	0.130 ± 0.015	^{127}Sn	29.8 ± 3.3	7560	{1.3 / 3.7}	0.44 ± 0.07
1131.5	1.25 ± 0.04	^{135}I	22.8 ± 0.5	23 796	18	5.48 ± 0.22
1180.6	0.176 ± 0.007	^{151}Nd	15.3 ± 1.0	746	4	1.15 ± 0.05
1230.7	0.0379 ± 0.0046	^{156}Eu	8.46 ± 0.60	1.31 *E*6	33 840	0.44 ± 0.06
1260.4	1.625 ± 0.050	^{135}I	29.0 ± 0.4	23 796	18	5.60 ± 0.19
1283.23 [q]	0.552 ± 0.065	^{139}Cs	7.7 ± 3.1 [q]	570	40	6.8 ± 2.8
1313.0	1.23 ± 0.28	^{136}I	68 ± 1	83	17	1.8 ± 0.5
1383.9	1.18 ± 0.04	^{92}Sr	90 ± 10	9756	4.5	1.31 ± 0.15
1428.3	1.50 ± 0.13	^{94}Sr	95.4 ± 0.4	75	2.7	1.52 ± 0.14

TABLE II. *(Continued)*

E_γ (keV) [a]	Yield per 100 fissions	Assigned fission product	Gamma-ray branching ratio (%) [b]	$T_{1/2}$ (s)	$T_{1/2}$ (parent) (s)	Cumulative fission product yield (%)
1435.9	4.36 ±0.29	^{138}Cs	76.3 ±1.6	1932	850	5.71 ±0.38
1525.4	0.36 ±0.05	^{146}Pr	18.3 ±2.2	1440	834	1.97 ±0.35
1596.6	5.33 ±0.16	^{140}La	95.4 ±0.08	1.15 *E*5	1.11 *E*6	5.58 ±0.17
1768.2	0.798 ±0.047	^{138}Xe	16.7 ±0.7	850	6.5	4.78 ±0.34
1836.0	0.140 ±0.011	^{88}Rb	21.4 ±1.2	1067	10296	0.58 ±0.06 [r]
1897.6	0.043 ±0.012	^{84}Br	14.9 ±1.8	1908	200	0.29 ±0.09

[a] Values given to 0.01 keV taken from Borner *et al.*, Ref. 26. Values given to 0.1 keV taken from *Table of Isotopes*, Ref. 27, except as indicated.
[b] Values taken from *Table of Isotopes*, Ref. 27, or our previous evaluation, Ref. 12, except as indicated.
[c] Estimated from data of Smither *et al.*, Ref. 28, and the evaluation of Kroger and Reich, Ref. 29.
[d] Values in parentheses may be in error. See text for discussion on these results.
[e] Hansen *et al.*, Ref. 30.
[f] Franz and Herrmann, Ref. 31.
[g] Schneider *et al.*, Ref. 32.
[h] Bjornstad *et al.*, Ref. 33.
[i] Uncertainty estimated from data of Matumoto and Tamura, Ref. 34.
[j] Recent results of Ikeda *et al.*, Ref. 43, indicate the existence of two ^{148}Pr isomers having half-lives of 2.3 and 2.0 min and having different branching ratios for the 302-keV transition. The separate contributions could not be determined for the present data.
[k] Uncertainty estimated from data of Fettweis and del Marmol, Ref. 35.
[l] Branching ratio from Harmatz, Ref. 36; uncertainty estimated from data given in Harmatz, Ref. 36.
[m] Estimated from data of Niizeki *et al.*, Ref. 37.
[n] Estimated from data of Skarnemark *et al.*, Ref. 38.
[o] Estimated from data of DeFrenne *et al.*, Ref. 39.
[p] Branching ratio from Blachot and Fiche, Ref. 40; uncertainty estimated from data given in Kim, Ref. 41.
[q] Lee and Talbert, Ref. 42.
[r] Cumulative fission yield of parent (^{115}Cd, ^{102}Mo, ^{114}Cd, ^{106}Ru, ^{97}Zr, ^{88}Kr).
[s] Independent yield.
[t] Branching ratio from Summerer *et al.*, Ref. 44; uncertainty estimated from data of Summerer *et al.*, Ref. 44.

sion product for each A between 84 and 156 but were not successful for A = 85, 86, 96, 98, 100, 116–126, 150, 154, and 155 because either the half-life of the searched for fission product was too short or else unambiguous gamma-ray assignments simply could not be made. For example, the 133-keV gamma ray from decay of ^{144}Ce was masked by the much stronger 133-keV transition following α decay of ^{245}Cm. Data reduction for ^{133}Xe and ^{133}Xe* was comprised by the slow nonradiative loss of these noble gases from the sample, the rate having been measured previously[12] as a loss of about 50% in 9 days, slow enough not to affect measurements for the heavier Xe isotopes reported in Table I, but fast enough to render data reduction unreliable for ^{133}Xe and ^{133}Xe*.

DATA ANALYSIS

To determine the yield C of a given fission product required knowledge of the nuclear properties, particularly the gamma-ray branching ratio, the half-life of the fission product, and the half-life of its parent. These are also tabulated in Table II. Many of these data had been evaluated for our ^{239}Pu measurements,[12] and most of the remaining data were obtained from the most recent *Table of Isotopes*.[27] For a few cases a reference to more current measurements[28–44] is quoted. Similar tables of fission-product nuclear data have been given by Theirens *et al.*,[21,45,46] but without uncertainties which are required for uncertainty assignments to the deduced fission yields. Nethaway *et al.*[47] and Nagy *et al.*[48] have also tabulated nuclear data to be used in fission yield determinations.

There were several gamma rays which were reliably assigned as decay of particular short-lived fission products for which absolute branching ratios are unknown. In these cases only the experimental gamma-ray yield/fission was determined and is reported.

The final column of Table II gives the deduced cumulative fission yields for the fission products listed in column 3, except for ^{136}Cs (an independent yield), except for those fission products for which the branching ratio B is not known, and except for those fission products for which the parent half-life is much longer than the daughter half-

life and data were such that the contribution due to independent creation of the daughter could not be determined. For the nuclides given in Table I, the least-squares calculation provided not only the independent yields but also the cumulative yields, and the latter had smaller absolute uncertainties than the former for most of the data. For data requiring application of Eqs. (3) and (4) estimates of the parent contribution were made from a graph plotting the fractional yields of Table I as a function of $Z - Z_{UCD}$ as discussed in the next section. The uncertainties quoted for the cumulative fission yields in the last column of Table II include all of the uncertainties quadratically combined except the ~7.7% overall normalization uncertainty.

As noted in the report[12] on ^{239}Pu fission yields, a problem with the determination of fission-product yields in the present manner is the reliance on nuclear data, particularly branching ratios, which could be in serious error. The latter situation appears to be the case for ^{148}Pr. The evaluated branching ratio in the *Table of Isotopes*[27] is $(90.9 \pm 0.4)\%$ and the half-life is 2.3 min. Recently, Ikeda *et al.*,[43] published results showing the creation of two isomers of ^{148}Pr in ^{235}U fission. For one isomer the half-life is (2.27 ± 0.04) min and the 302-keV transition has a branching ratio of ≈60%; for the other isomer the half-life is (2.0 ± 0.1) min and the 302-keV transition is ≈100%. It is impossible, therefore, to determine the ^{148}Pr yield from the present measurement of the yield/fission of the 302-keV gamma ray. Consequently, we were not able to obtain an $A = 148$ chain yield. Gamma-ray branching ratios for other short-lived fission products were similarly investigated if either the absolute value for the branching ratio was not available in the literature or else was in doubt. In the next section results and discussion for 22 gamma rays are given. To conclude this section, we report that the nuclear data in Table II have been subjected to careful review, and given the present state of knowledge, appear to be correct.

DISCUSSION

Necessary to complete the task of determining chain mass (A) distributions are the charge distributions for all mass chains. These would be very difficult to obtain experimentally. Studies[4,22] of representative data particularly for $n_{th} + ^{235}$U and ^{252}Cf(s.f.) indicate that the charge distribution for a given A may be represented by a Gaussian distribution having a most probable charge $Z_p(A)$ and a width parameter $\sigma(A)$; the fractional cumulative yields of fission products for a given A are related by

$$\sum_{1}^{Z} F(Z) = \frac{1}{\sigma(2\pi)^{1/2}} \int_{-\infty}^{Z+1/2} \exp \frac{-(n - Z_p)^2}{2\sigma^2} dn . \quad (6)$$

Analyses[4,22] of representative data sets for several fissioning systems indicate $\sigma \simeq 0.6$ will give satisfactory results when used in Eq. (6). These analyses also indicate that, at least empirically, one may relate Z_p for different fissioning systems.[49] In actual practice, there are rarely sufficient data to obtain Z_p and σ values from Eq. (6) for each A. Instead, an approximation to $Z_p(A)$ is computed using, e.g., the unchanged charge distribution (UCD) hypothesis,[22] an hypothesis that assumes that no redistribution of charge occurs during fission and which was first suggested to explain high-energy fission.[50] Then such fractional cumulative yields as have been determined are plotted versus $(Z - Z_{UCD})$. In this hypothesis

$$Z_{UCD}(A) = (Z_F / A_F)(A + \nu_A) . \quad (7)$$

Z_F and A_F are the charge and mass, respectively, of the fissioning nucleus, and ν_A is the number of neutrons emitted by the corresponding fission fragment and is estimated[22] from

$$\nu_h = 0.531\nu + 0.062(A_h - 143) , \quad (8a)$$

$$\nu_l = 0.531\nu + 0.062(A_l + 143 - A_F) , \quad (8b)$$

for heavy and light-mass fragments where ν is the average number of neutrons emitted during fission. For ^{245}Cm thermal-neutron fission[51] $\nu = 3.832(\pm 1\%)$. Fractional cumulative yields determined from the present data are shown in Fig. 4 plotted on a probability scale versus $Z - Z_{UCD}$. The solid points indicate data derived from a least-squares analysis using Eq. (1), and the open circles indicate values obtained from separate determinations of parent and daughter nuclides, and have generally larger error bars. Four lines are shown in this figure, including one showing results[4] of analysis for $n_{th} + ^{235}$U fission and one showing results[4] of analysis of ^{252}Cf spontaneous fission. The slopes of these two lines are essentially the same, $\sigma \simeq 0.6$. The present data for the heavy masses are reasonably well represented by the ^{252}Cf curve; to get a slightly better fit, we assumed $\sigma = 0.6$ and obtained the heavy solid line. The heavy dashed line was estimated to represent the light-mass data assuming $\sigma = 0.6$. The separation of ~ one unit in Z_{UCD} between the heavy dashed and heavy solid lines is in agreement with the estimate of Wahl *et al.*,[52] based on other fissioning systems.

Recently, Gindler[53] has discussed the problem of determining the number of neutrons emitted as a function of fragment mass for several fissioning systems, including $n_{thermal} + ^{245}$Cm. For the purpose of the present report, we note that the number of neutrons emitted by a fission fragment computed

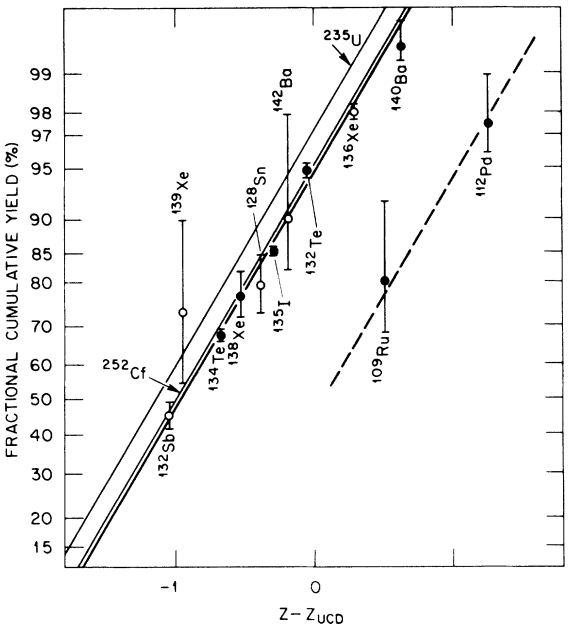

FIG. 4. Fractional cumulative yields for thermal-neutron fission of ^{245}Cm plotted on probability scale versus $Z - Z_{UCD}$. The heavy-mass data are well represented by the heavy line on this figure. The fact that the heavy line is linear in this representation means that the Gaussian width parameter for Eq. (6) is independent of A. Two light lines labeled ^{235}U and ^{252}Cf indicate similar analysis for $n_{th}+^{235}$U and ^{252}Cf (s.f.), respectively. There are only two data available for light masses, and the heavy dashed line indicates the best estimate under these circumstances for the dependence of the fractional cumulative yield on $Z - Z_{UCD}$.

using Eq. (8a) or (8b) approximates closely the number determined by Gindler[53] for the important mass regions. Using ν_A determined by Gindler[53] would not appreciably alter the results shown in Fig. 4.

Having thus determined a reasonable representation of charge distribution applicable to the heavy masses, and assuming that the light masses are satisfactorily represented by the dashed line in Fig. 4, the fission-product yield data of Table II were analyzed to obtain the best values for total chain yields. When only one isotope of a given mass chain was studied, its fractional cumulative yield was determined from Fig. 4. For example, for ^{144}La, $(Z - Z_{UCD}) = -0.13$, and the fractional cumulative yield from Fig. 4 is 0.945. Hence the $A = 144$ chain yield is ~6% larger than the fission-product yield for ^{144}La. For those A for which there were several fission products measured, or several gamma rays for the same fission product, a "best" value was determined by weighted averaging including corrections for <1.0 fractional cumulative yields as discussed for ^{144}La. Derived values for chain yields are given in Table III in the columns labeled "Measured." The columns labeled "Inferred" are estimates based either on previous measurements[5,6] or best guesses from interpolations of the measured values. A 20% uncorrelated uncertainty was assigned to individual inferred values obtained from the interpolation. The separate columns were summed as indicated at the end of the table, and the measured sums were added to the inferred sums. The quoted relative uncertainties were combined quadratically, which may underestimate the uncertainties quoted with the sums. The "Total" sums are very close to 100% for the total light-mass and for the total heavy-mass yields. There are very satisfactory results, well within the rather large 7.7% experimental uncertainty associated with determination of the number of fissions.

A. Comparisons of cumulative fission yields

As mentioned in the Introduction, prior measurements of fission yields for $n_{th}+^{245}$Cm utilized the comparison method for determining fission-product yields. The technique is to irradiate samples of ^{245}Cm and ^{235}U simultaneously, and then to determine individual fission product activities R from each sample in as nearly identical manner as possible. One then obtains the yield for the ^{245}Cm measurement, Y_{245}, from this technique by calculating

$$Y_{245} = \frac{R_{245}}{R_{235}} \frac{(N\sigma_f)_{245}}{(N\sigma_f)_{235}} Y_{235} \tag{9}$$

for each separate activity, where $(N\sigma_f)$ represents the number of fissions created in the sample. The ratios of activities, R_{245}/R_{235}, are the prime experimental data in these experiments, and the reported[5-7] measured uncertainties on these ratios are small. Reported uncertainties in the ratio of the $(N\sigma_f)$ are likely underestimated; however, they affect only the total normalization and, as discussed above, may not be important. The values of and uncertainties associated with the Y_{235} are the most important. In fact, one difficulty in comparing the separate data sets[5-7] is associated with the slightly differing values for individual Y_{235} and ΔY_{235} used by the several authors. However, overall the values of Y_{235} used are not very different from those in current evaluations.[1,2,54] In Table IV we present the data deduced from the present experiment for comparison with the data from prior experiments as originally reported.

Some care should be exercised in comparing the data sets in Table IV. The uncertainties associated with the ANL data set[6] appear to be absolute total uncertainties, including normalization uncertainty. The Savannah River Laboratory (SRL)

TABLE III. Chain yields (%) for thermal-neutron fission of ^{245}Cm.

Mass	Measured	Inferred	Mass	Measured	Inferred
≤83		1.0 ±0.50	122–126		0.43 ± 0.20
84	0.29 ± 0.09		127	0.426 ± 0.035	
85		0.31 ± 0.04 [a]	128	0.68 ±0.05	
86		0.37 ± 0.10	129	1.06 ±0.12	
87	0.50 ± 0.04		130	1.94 ±0.15	
88	0.58 ± 0.06		131	2.82 ±0.08	
89	0.82 ± 0.09		132	4.19 ±0.12	
90	1.15 ± 0.28		133	5.39 ±0.16	
91	1.18 ± 0.07		134	5.81 ±0.21	
92	1.31 ± 0.15		135	6.34 ±0.16	
93	1.93 ± 0.19		136	6.30 ±0.30	
94	1.68 ± 0.12		137	5.3 ±1.2	
95	2.31 ± 0.08		138	6.00 ±0.20	
96		2.55 ± 0.51	139	6.6 ±1.2	
97	2.92 ± 0.10		140	5.51 ±0.14	
98		3.45 ± 0.69	141	5.38 ±0.16	
99	4.10 ± 0.13		142	4.67 ±0.26	
100		4.80 ± 0.96	143	4.40 ±0.24	
101	5.70 ± 0.52		144	4.56 ±0.33	
102	5.8 ±1.2		145	3.04 ±0.27	
103	6.19 ± 0.14		146	2.79 ±0.12	
104	6.67 ± 0.40		147	2.57 ±0.13	
105	6.43 ± 0.21		148		2.15 ± 0.43
106	5.7 ±0.4		149	1.94 ±0.15	
107	5.5 ±0.5		150		1.50 ± 0.30
108	5.8 ±1.5		151	1.16 ±0.06	
109	3.76 ± 0.52		152	1.4 ±0.7	
110		3.95 ± 0.79	153	0.77 ±0.62	
111	3.7 ±0.9		154		0.65 ± 0.13
112	3.49 ± 0.43		155		0.53 ± 0.11
113		2.02 ± 0.50 [b]	156	0.44 ±0.06	
114	2.4 ±0.9		≥157		2.0 ±1.0
115	0.57 ± 0.03				
116–121		0.46 ± 0.20			
Sums	80.48 ± 2.62	18.91 ± 1.69		91.49 ±2.11	7.26 ± 1.16
Total	99.39 ± 3.12			98.75 ± 2.41	

[a] Harbour and MacMurdo, Ref. 5, report (0.29 ± 0.02) % for the yield of ^{85}Kr*.
[b] Value for ^{113}Ag reported by von Gunten *et al.*, Ref. 6.

data set[5] includes uncertainties in the ratio measurements and uncertainties in the Y_{235} used, but not overall normalization uncertainties. The latter were not given in their report. For the Bhabha Atomic Research Centre (BARC) data set[7] normalization was obtained by determining a complete mass distribution curve (by reflection about symmetric fission) and normalizing to 200%. These authors suggest the overall errors in their yield data should be 5–10%. Since 5–10% is larger than many of the ΔY_{245} given for the BARC data in Table IV, it must be assumed that there is a minimum overall normalization uncertainty of 5% associated with these data in addition to the quoted uncertainties. Relative errors are assigned to the present values in Table IV and are comparable to relative errors given for the previous measurements.[5-7]

The ANL, SRL, and BARC data sets are correlated through the Y_{235} and ΔY_{235} and any averaging procedure of these data sets should be cognizant of these correlations. The present data are not correlated with earlier data, except through the use of ^{245}Cm fission cross sections, and even these correlations may be unimportant since the absolute normalization of these several data sets relies directly or by inference upon good agreement with a total of 200% for the mass yields. The major conclusion from comparison of the present data with prior data in Table IV is that all of the data sets are in reasonable agreement for most of the fission product yields within assigned uncertainties.

TABLE IV. Comparisons of cumulative fission product yields for thermal-neutron fission of ^{245}Cm.

Fission product	ANL (1967) [a]	SRL (1972) [b]	BARC (1979) [c]	ORNL (1980)
^{88}Kr		0.61 ± 0.04		0.58 ± 0.06
^{89}Rb	0.85 ± 0.10 [d]		0.82 ± 0.02 [d]	0.82 ± 0.09
^{91}Sr		1.11 ± 0.02	0.93 ± 0.02	1.18 ± 0.06
^{92}Sr		1.25 ± 0.11		1.31 ± 0.15
^{93}Y		1.75 ± 0.11		1.93 ± 0.19
^{95}Zr	2.40 ± 0.30	2.36 ± 0.06	2.14 ± 0.19	2.35 ± 0.19
^{97}Zr	3.10 ± 0.35	3.00 ± 0.06	2.89 ± 0.08	2.92 ± 0.09
^{99}Mo	4.18 ± 0.40	4.09 ± 0.12	4.00	4.10 ± 0.13
^{103}Ru	6.27 ± 0.90	5.85 ± 0.42	6.55 ± 0.40	6.18 ± 0.19
^{105}Ru	5.78 ± 1.20			6.43 ± 0.21
^{106}Ru	5.75 ± 1.40			5.7 ± 0.4
^{109}Pd	5.23 ± 0.60			3.76 ± 0.52 [e]
^{111}Ag	3.63 ± 0.70	3.93 ± 0.20	3.84 ± 0.20	3.7 ± 0.9
^{112}Pd	1.60 ± 0.40			3.42 ± 0.43
^{115}Cd	0.41 ± 0.07		0.38 ± 0.01	0.57 ± 0.03
^{127}Sb	0.57 ± 0.09		0.45 ± 0.10	0.43 ± 0.04
^{129}Sb	1.42 ± 0.30			1.06 ± 0.12
^{131}I	3.18 ± 0.40	2.90 ± 0.08	2.93 ± 0.02	2.82 ± 0.08
^{132}Te	4.41 ± 0.80	3.85 ± 0.09	3.74 ± 0.05	4.01 ± 0.11
^{133}I	6.01 ± 0.70	5.52 ± 0.08	5.34 ± 0.09 [f]	5.39 ± 0.16
^{135}Xe		6.27 ± 0.30 [g]	6.90 ± 0.01	6.06 ± 0.24
^{138}Cs		6.01 ± 0.22		5.71 ± 0.38
^{139}Ba		5.52 ± 0.33		6.6 ± 1.2
^{140}Ba	5.70 ± 0.70	5.36 ± 0.08	5.54 ± 0.22	5.39 ± 0.16
^{141}Ce	5.20 ± 0.70	5.10 ± 0.13	4.99 ± 0.06	5.38 ± 0.16
^{142}La		4.84 ± 0.08		4.67 ± 0.28
^{143}Ce	3.85 ± 0.60	4.39 ± 0.07	4.42 ± 0.03	4.40 ± 0.24
^{147}Nd	2.60 ± 0.50	2.18 ± 0.05	2.50 ± 0.03	2.57 ± 0.13
^{149}Nd	1.97 ± 0.40 [h]			1.94 ± 0.15
^{151}Pm	1.35 ± 0.35			1.18 ± 0.08
^{156}Eu	0.25 ± 0.06			0.44 ± 0.06

[a] Von Gunten, Flynn, and Glendenin, Ref. 6.
[b] Harbour and MacMurdo, Ref. 5.
[c] Ramaswami *et al.*, Ref. 7.
[d] Data for ^{89}Sr.
[e] Data for ^{109}Rh.
[f] Data for ^{133}Xe.
[g] Data for ^{135}I + ^{135}Xe.
[h] Data for ^{149}Pm.

B. Comparison of independent fission yields

In Table V are data for independent fission yield measurements compared with previously reported data.[6,8-11] The present data are in good agreement with ANL[6] and SRL[10,11] data, but in definite disagreement with recent BARC measurements.[8,9] The discrepancy is of some concern because the BARC values suggest a much smaller value for the Gaussian width parameter (σ) for $A = 135$ and at the same time a much larger value for this parameter for $A = 140$ than $\sigma \simeq 0.6$ expected from analyses of other fissioning systems. If the BARC values are closer to true values than the present data (due to some error in the present experiment) for these fractional yields, then the use of the data in Fig. 4 to determine the mass yields in Table III from the fission product yields in Table II could be in error for those cases requiring a correction as described above for ^{144}La. In addition, the use of the results of Fig. 4 to estimate C_p^c in Eq. (3) when required could result in incorrect values for C_d^i, leading to an error in C_d^c using Eq. (4). We emphasize that the use of Fig. 4 for the present experiment is primarily for the purposes just stated, i.e., to determine fractional yields when needed in the analysis of the data. Although the present results as shown in Fig. 4 are consistent with a constant width parameter σ and with representing $Z_p(A)$ as a simple function of A, they are not sufficient to specify that these are the only descriptions of σ and $Z_p(A)$. It has long been

TABLE V. Comparisons of fractional fission product yields for thermal neutron fission of ^{245}Cm.

Fission product	ANL (1967) [a]	SRL (1971) [b]	BARC (1980) [c]	ORNL (1980)
^{132}Te		0.94 ± 0.01		0.948 ± 0.005
^{134}Te		0.59 ± 0.07 [d]		0.68 ± 0.02 [d]
^{135}I		0.83 ± 0.02	0.951 ± 0.014	0.854 ± 0.006
^{136}Cs	0.16 ± 0.03 [e]			0.13 ± 0.01 [e]
^{140}Ba			0.969 ± 0.006	0.994 ± 0.003

[a] Von Gunten, Flynn, and Glendenin, Ref. 6.
[b] Troutner and Harbour, Ref. 10; Harbour, Troutner, and MacMurdo, Ref. 11.
[c] Datta *et al.*, Ref. 8; also Singh *et al.*, Ref. 9.
[d] Ratio of Te to Te + I.
[e] Independent yield of shielded fission product.

suggested[55] that for $n_{\text{thermal}} + ^{235}$U, σ is not constant and $Z_p(A)$ is an irregular function of A, and that there are odd-even effects.[52] However, even for this well-known reaction there are insufficient data to determine all of the required $Z_p(A)$ and $\sigma(A)$.

For $n_{\text{thermal}} + ^{245}$Cm, the present experiment provides a substantial fraction of the known yield data for this system, and these data are not sufficient to provide any further theoretical insight than suggested above. The present data are in good agreement with prior measurements (Tables IV and V) *except* for the fractional fission yields of ^{135}I and ^{140}Ba. These discrepancies are too large to ignore, in particular, since the measurements are quite similar. However, the method of analysis of the data by the BARC group is different from our method. Our method is a least-squares calculation using Eq. (1) as a basis. We indicate this calculation for ^{140}Ba → ^{140}La → ^{140}Ce. Let $\vec{I}$ be a two-component vector representing the initial concentrations of ^{140}Ba and ^{140}La, namely $I_1 = n_f C_p^c(^{140}\text{Ba})$ and $I_2 = n_f C_d^i(^{140}\text{La})$ in Eq. (1). Let $\vec{D}$ be the n-component vector representing the experimental gamma-ray yields given by $[(Y/\epsilon)/B]$ in Eq. (1). Let $\vec{V}_{\vec{D}}$ be the $n \times n$ covariance array of these data. Finally let $\vec{G}$ be the $2 \times n$ array containing $\partial D_i / \partial I_j$. Then[56]

$$\vec{I} = (\vec{G}^+ \vec{V}_{\vec{D}}^{-1} \vec{G})^{-1} \vec{G}^+ \vec{V}_{\vec{D}}^{-1} \vec{D} \qquad (10a)$$

and

$$\vec{V}_{\vec{I}} = (\vec{G}^+ \vec{V}_{\vec{D}}^{-1} \vec{G})^{-1}, \qquad (10b)$$

where $\vec{V}_{\vec{I}}$ is the 2×2 covariance matrix of $\vec{I}$. This formalism is exact in the least-square's sense since Eq. (1) is linear in I_1 and I_2. This is the formalism used to determine the fractional yields and uncertainties given in Table I, and the cumulative yields and uncertainties given in Table II for the daughter nuclides in Table I. In particular, the uncertainties quoted in Tables I and II make use of the full covariance $\vec{V}_{\vec{I}}$ determination. In Fig. 5 we show results of analysis of our ^{140}Ba → ^{140}La → ^{140}Ce, $E_\gamma = 1596$ keV data, plotted to exhibit comparisons of the data with three different sets of initial concentrations of ^{140}Ba and ^{140}La. Because these three sets of initial conditions are not very different (unlike the data and calculations shown in Fig. 3), a ratio representation was chosen. The data (given by experimental points and uncertainties) and the calculated curves are plotted as a ratio to the best-fit calculation. Although application of Eqs. (10a) and (10b) result in a calculated initial ^{140}La fractional yield of 0.6% (±34%), subjective appraisal of Fig. 5 could support initial ^{140}La fractional yields between 0 and 2% as being almost as likely as 0.6%. However, the BARC value of (3.1 ± 0.6)%

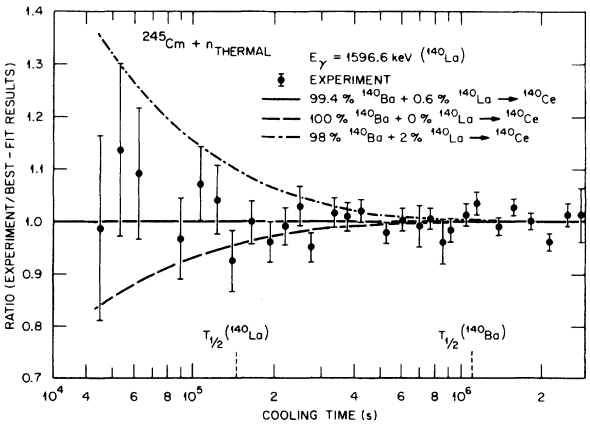

FIG. 5. Analysis of the decay of the 1596.6-keV gamma ray assigned to decay of ^{140}La, indicating the initial concentrations of ^{140}Ba and ^{140}La. The data and calculations are plotted as ratios (see Fig. 3 for the conventional plot) to enhance the vertical scale. Also shown are two calculations for two other sets of initial concentrations.

for the initial ^{140}La fractional yield is not quite consistent with the present measurements.

A possible explanation for the apparent difference in the reported ^{140}La fractional yields may be related to a subtle and generally unrecognized difference between the standard linear least-squares data-reduction methods[57] and the least-squares method given by Eqs. (10a) and (10b). The BARC group[8] used a graphical technique, based upon the linear functional dependence of I_1 and I_2. If both sides of Eq. (1) are divided by

$$\exp(-\lambda_d T)[1-\exp(-\lambda_d t_c)]$$

the resulting relationship I_1 and I_2 can be written as

$$Y = XI_1 + I_2 , \tag{11}$$

where the symbol "Y" has been redefined to agree functionally with that used in Ref. 8. Then

$$Y = A\exp(\lambda_d T)[1-\exp(-\lambda_d t_c)]^{-1} \tag{12a}$$

and

$$X = \frac{\lambda_p}{\lambda_p-\lambda_d} - \frac{\lambda_d}{\lambda_p-\lambda_d}\frac{\exp(-\lambda_p T)[1-\exp(-\lambda_p t_c)]}{\exp(-\lambda_d T)[1-\exp(-\lambda_d t_c)]}, \tag{12b}$$

where the symbol A in Eq. (12a) equals $[(Y/\epsilon)/B]$ in Eq. (1). Equations (12a) and (12b) are equivalent to Eqs. (2) and (3) of Ref. 8 for short irradiation; i.e., t (of Ref. 8) $\rightarrow 0$ [except for a missing t in the numerator of Eq. (2) of Ref. 8 which does not affect the analysis or the results]. From Eq. (11)

$$I_1 = dY/dX \tag{13a}$$

and

$$I_2 = Y(X=0) . \tag{13b}$$

To get the slope dY/dX and the intercept $Y(X=0)$, values of Y versus X are plotted, and a straight line is drawn through the points. In actual practice, the slope and the intercept are computed using standard linear least-squares techniques. In principle, such calculation should parallel that given by Eqs. (10a) and (10b), where now the $\vec{D}$ array will represent the Y of Eq. (12a), and the $\vec{G}$ array has one column given by the X of Eq. (12b) and the other column by a unit vector. The covariance matrix $\vec{V}_{\vec{D}}$ will be modified according to the extra terms containing T and t_c of Eq. (12a). We point out that the standard method of determining coefficients for linear least-squares regression analysis is equivalent to using the formalism of Eqs. (10a) and (10b) for which the covariance matrix $\vec{V}_{\vec{D}}$ *is set equal to the identity matrix*. If this is what was done in the analysis of the BARC data for ^{140}Ba $\rightarrow$ ^{140}La $\rightarrow$ ^{140}Ce, then the uncertainties in the experimental gamma-ray yields were not included in the analysis. Including the uncertainties in the analysis would not only result in a larger value for the uncertainty associated with the calculated ^{140}La fractional yield than quoted in Ref. 8 but could alter the calculated yield as well.

The discrepancy between the present results for the ^{135}I $\rightarrow$ ^{135}Xe $\rightarrow$ ^{135}Cs and the BARC results[8] for this decay chain appear to be too large to be accounted for by the above explanation. To ensure that the graphical technique does not contribute to an unsuspected difference in the analysis, the present data were also analyzed by this technique. The results are shown in Fig. 6. In this figure, which may be compared with Fig. 1 of Ref. 8, the line is the "best fit" representation of the plotted data, and when the slope and intercept are obtained, the results for the ^{135}Xe fractional yield are the same as those in Table I. The dashed line in Fig. 6 is one possible line which when similarly analyzed yields 95% for the ^{135}I fractional cumulative yield. The present data clearly do not support this much larger value for the ^{135}I fractional cumulative yield. We have, therefore, carefully analyzed the complete $A=135$ data reduction for a clue to the discrepancy between the two values for the ^{135}I fractional cumulative yield.

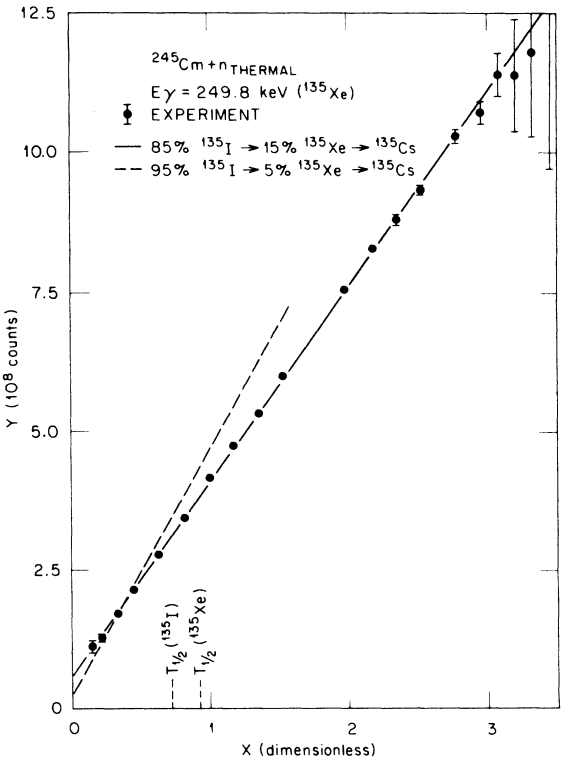

FIG. 6. Analysis of the decay of the 249.8-keV gamma ray assigned to decay of ^{135}Xe. This plot shows the relationship between Y of Eq. (12a) and X of Eq. (12b). The dashed curve indicates a calculation using a different set of initial concentrations.

The relevant part of the decay chain for $A=135$ is

$$^{135}\text{Te} \xrightarrow{\beta^-} {}^{135}\text{I} \begin{cases} \xrightarrow{\beta^-} {}^{135}\text{Xe}^* \ (T_{1/2}=15.6 \text{ min}) \\ \xrightarrow{15\%} \text{I.T. (527 keV)} \\ \xrightarrow{\beta^-} {}^{135}\text{Xe} \xrightarrow{\beta^-} {}^{135}\text{Cs}. \end{cases}$$

We observed the 526.6-keV gamma ray from the decay of ^{135}Xe* and obtained the fraction of ^{135}Xe* independent yield (see Table I) and the gamma-ray yield/fission (see Table II). The additional complication due to time dependence of the ^{135}Xe ground-state decay has in the past been assumed to be negligible.[8,19] We checked this aspect carefully by determining the complete formula for the ^{135}Xe decay time dependence equivalent to Eq. (1) (i.e., for short irradiation period). For $T \gg T_{1/2}(^{135}\text{Xe}^*)$, the correction to results obtained using Eq. (1) due to the independent yield of ^{135}Xe* is <0.5%.

Another possible correction, due to thermal-neutron capture by ^{135}Xe ($\sigma_{\text{capt}} \sim 3.6*10^6$ b[58]) during the irradiation was investigated. During the irradiation the total decay constant becomes

$$\lambda_{\text{total}} = \lambda_{\text{decay}} + N\sigma_{\text{capt}}, \tag{14}$$

where N is the incident neutron flux. In our case $N\sigma \sim 5 \times \lambda_{\text{decay}}$. However, for $t_{\text{irrad}}=40$ s, $N\sigma t_{\text{irrad}} \sim 2 \times 10^{-4}$, and so the deduced independent yield of ^{135}Xe is not affected by loss of ^{135}Xe by thermal-neutron capture during the irradiation.

A third possible source of error is a nonradiative loss of ^{135}Xe from the source, e.g., by diffusion or escape through a pinhole. We have encountered this problem in the past.[12,14] We were not able to extract results for the 81-keV gamma ray from decay of 5.3-d ^{133}Xe from the present spectral data because of a large Compton continuum from x rays following α decay of ^{245}Cm. However, the ^{245}Cm sample was prepared as nearly identical as possible to the preparation of the sample for the ^{239}Pu measurements,[12] and in those measurements the ^{133}Xe nonradiative loss rate was determined to be ~50% in 9 days, a loss rate in rough agreement with diffusion of Xe through the walls of the polyethylene transport capsule.[14] It is not likely that ^{135}Xe escaped from our sample during the ~24 hours of measurements in sufficient quantities to affect our results. But, if there were ^{135}Xe escape, this would reduce the apparent independent ^{135}Xe fission yield that we report. The possibility of ^{135}I escape was also studied previously[14] with negative results.

Finally, as a check on the internal consistency of our results we compare the calculated ^{135}I cumulative fission yields determined from analysis of the 527-keV decay of ^{135}Xe* and 250-keV decay of ^{135}Xe with those determined from the prominent 1132- and 1260-keV gamma rays from decay of ^{135}I. These cumulative fission yields are as follows:

(a) FCY = 5.48 ± 0.22 for E_γ = 1132 keV,
(b) FCY = 5.60 ± 0.19 for E_γ = 1260 keV,
(c) FCY = 5.36 ± 0.31 for E_γ = 527 keV,
(d) FCY = 5.19 ± 0.23 for E_γ = 250 keV.

The value (d) is the smallest, but not significantly so, and could be due to the possibility that the branching ratio (B) of (90 ± 3)%[27] for the 250-keV gamma ray from decay of ^{135}Xe is too large.

In summary, the present measurements have been thoroughly reviewed, and several likely sources of error have been carefully scrutinized. Our fractional yield value for $A=135$ agrees with the earlier SRL datum,[10,11] which agreement is comforting but not sufficient to exclude completely the possibility of an undetected error in the present experiment. Resolution of this discrepancy may await further experimental results.

C. Comparison of mass distributions

Derived values of chain yields are plotted in Fig. 7 compared with curves representing evaluations for ^{239}Pu (Ref. 2) and ^{252}Cf (Ref. 4). The results for the $n_{\text{th}}+^{245}$Cm measurements lie between those for $n_{\text{th}}+^{239}$Pu and ^{252}Cf spontaneous fission. The heavy mass distribution appears to be influenced by the $Z=50$ (Sn) and $N=82$ shell closures, not as marked as for the ^{240}Pu fissioning system, but much more apparent than for the ^{252}Cf fissioning system. The light mass distribution may indicate a weak contribution of the $Z=40$ (Zr) and $N=50$ shell closures. It is also possible that the present values indicate fine structure effects similar to those observed for lighter fissioning systems.

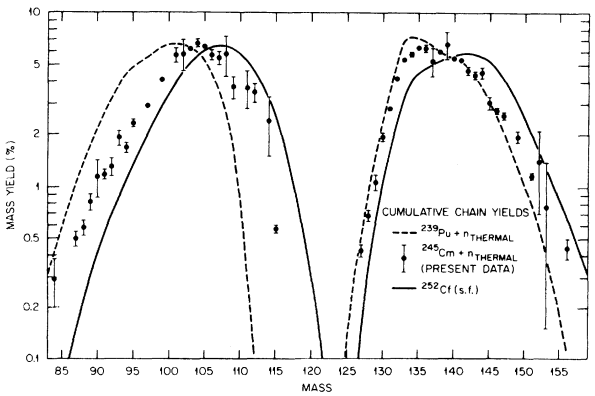

FIG. 7. Mass-yield distribution for $n_{\text{thermal}}+^{245}$Cm derived from the present measurements. Also shown for comparison are smoothed curves representing $n_{\text{thermal}}+^{239}$Pu and ^{252}Cf spontaneous fission mass distribution.

D. Absolute gamma-ray branching ratios

As mentioned at the end of the last section, because of concern for the accuracy of the nuclear data required to deduce fission yields, all of these data were scrutinized carefully. Particularly for the short-lived fission products, newly available results were included in the analyses, as indicated by the footnotes of Table II. Having deduced mass distributions assuming accuracy of the nuclear data, it is reasonable to consider the inverse, that is, to assume accuracy of the mass distributions of Table III and then to deduce gamma-ray emission probabilities in the decay of given fission products. Because there are data available, the same reverse analysis can be done for ^{252}Cf (s.f.). Wilhelmy's thesis[59] lists >500 gamma rays and their half-lives and gamma rays/fission for ^{252}Cf (s.f.) for $41 < E_\gamma < 724$ keV. Many, but not all, of these data were ascribed (sometimes tentatively) to decay of specific fission products. The latest Rider and Meek[1] evaluation includes recommended cumulative fission product yields and uncertainties for ^{252}Cf. (s.f.) which may be combined with Wilhelmy's gamma-ray yield data to determine branching ratios for specific gamma rays.

All of these data are collected in Table VI for 22 gamma rays for short-lived fission products, including four fission products (^{109}Ru, ^{110}Rh, ^{111}Rh, and ^{133}Sb) for which absolute gamma-ray branching ratios have not previously been determined. For the columns labeled "Present data" the gamma-ray yields were taken from Table II, and the mass yields were taken from Table III *except* for mass yields deduced from gamma-ray data due to decay of the fission product in column 1 for that mass. For example, analysis for ^{107}Rh is not included in the "Present data" because the mass yield for $A = 107$ was deduced from data in Table II for ^{107}Rh. However, data exist in the ^{252}Cf (s.f.) compilation for ^{107}Rh, and it is of interest to compare the deduced branching ratio for the 303-keV gamma ray with that given in Table II and used in the present $A = 107$ chain yield analysis. The data in the column labeled "Estimated FCY" were obtained from the fractional cumulative yield curves in Fig. 4. The sixth column gives the deduced gamma-ray branching ratios. For the ^{252}Cf (s.f.) analysis, the seventh column gives data from the tabulation in Wilhelmy's report[59] when it was identified in that report, or when it was apparent from the measured half-life, that an unidentified gamma ray was almost surely from decay of the chosen fission product. The eighth column contains the Rider and Meek[1] recommended yields for the specific fission products. The ninth column contains the deduced branching ratios. The last column of Table VI gives the branching ratios in the *Table of Isotopes*.[27] Some are the results of evaluations by one of the seven authors of the *Table of Isotopes*; others (in column ten) are the results of the most recent, or else the preferred, experiment; a few are estimates.

For the four isotopes mentioned at the beginning of the last paragraph, the best agreement between the ^{245}Cm and the ^{252}Cf analysis occurs for ^{110}Rh, and an average of these two results suggests a branching ratio for $E_\gamma = 373.8$ keV to be $(51 \pm 8)\%$. For ^{111}Rh the uncertainty associated with the ^{245}Cm-derived branching ratio is very large; the ^{252}Cf-derived branching ratio is suggested. For ^{109}Ru, the two branching ratios plus uncertainties just overlap. An average of these results suggests a branching ratio of $(26 \pm 6)\%$ for $E_\gamma = 206.2$ *if* the 206.2-keV gamma ray belongs to decay of ^{109}Ru as suggested by Franz and Herrmann.[31] A difficulty with this assignment is that this gamma ray is not reported at all in the experiment on the decay of ^{109}Ru by Fettweis and del Marmol.[35] For ^{133}Sb, the ^{245}Cm-derived value is preferred until a more definitive study on this nuclide is performed.

CONCLUSION AND RECOMMENDATIONS

The goal of the present experiment was to provide a large body of data on fission-product yields for thermal-neutron fission of ^{245}Cm. More data, in particular the results given in Table I for independent yields of daughter nuclides, were obtained than had been originally anticipated. The strong points of the present experiment follow: (a) It is essentially an independent measurement having only the ^{245}Cm fission cross sections in common with prior experiments; and (b) since chemical separations are not used, relative normalization uncertainties among yields for different fission products are reduced. Although the basic spectral data, as exhibited in Figs. 1 and 2, appear quite complicated, for most of the gamma rays given in Table II data reduction was not unusually difficult, and the observed deviation of an individual datum generally was smaller than expected statistical fluctuations. The major weakness in determining fission yields by this technique is the need to rely on nuclear data, and as indicated several times above, such data need to be carefully reviewed. Continued improvement in accuracy and precision of nuclear data should be encouraged.

ACKNOWLEDGMENTS

We wish to thank J. E. Bigelow and personnel of the ORNL TRU facility for providing the ^{245}Cm sample free of fission products and other actinides. We also appreciate very much the efforts of K. J.

TABLE VI. Gamma-ray branching ratios for selected short-lived fission products.

Fission product	E_γ (keV)	Present data for ^{245}Cm γ-ray yield (%/fission)	Mass yield (%/fission)	Estimated[a] FCY (%)	Branching ratio (%)	^{252}Cf (s.f.) data γ-ray yield[b] (%/fission)	Rec. F. P. yield[c] (%/fission)	Branching ratio (%)	Evaluated[d] branching ratio (%)
^{103}Tc	346.2	1.14 ±0.14	6.19±0.14	100	18.4± 2.3	0.9 ±2.7			
^{105}Tc	143.3	0.98 ±0.05	6.43±0.21	97	15.7± 1.0	0.9 ±1.4			11 ±1
^{107}Rh	302.8					4.06 ±1.06	6.52±0.52	62 ±17	65.9±4.6
^{108}Ru	165.0					1.66 ±0.05	5.95±0.65	27.9± 3.2	28 ±7
^{109}Ru	206.2	0.91 ±0.09	3.76±0.52	80	30.3± 5.1	1.14 ±0.14	5.27±1.21	21.6± 5.6	
^{109}Rh	326.7					3.42 ±0.50	5.95±0.65	58 ±11	62
^{110}Rh	373.8	2.0 ±0.2	3.95±0.79	96	53 ±12	2.58 ±0.25	5.12±0.82	50 ±10	
^{111}Rh	275.3	2.8 ±1.5	3.7 ±0.9	80	95 ±56	2.88 ±0.23	5.02±0.55	57 ± 8	
^{113}Ag	298.4	0.18 ±0.02	2.0 ±0.5	100	8.9± 2.4	0.76 ±0.34	3.12±0.19	24 ±11	9
^{114}Ag	558.0					1.75 ±0.10	3.45±0.79	51 ±12	≈10
^{133}Sb	1096.2	0.40 ±0.06	5.39±0.16	21	35 ± 6				
^{137}I	600.5	0.09 ±0.04	5.3 ±1.2	40	4.3± 2.1				6.8±2.3
^{137}Xe	455.5					1.47 ±0.03	4.69±0.38	31.4± 2.6	31 ±3
^{139}Xe	218.8	2.39 ±0.18	6.6 ±1.2	51	71 ±14	2.36 ±0.03	3.88±0.43	61 ± 7	50 ±6
^{139}Cs	1283.2	0.552±0.065	6.6 ±1.2	95	8.8± 1.9				7.3±0.6
^{140}Cs	602.4	2.61 ±0.15	5.51±0.14	85	55.7± 3.5	2.94 ±0.94	5.58±0.16	53 ±17	72 ±3
^{141}Ba	343.7	0.569±0.042	5.38±0.16	96	11.0± 0.9	0.882±0.016	6.13±0.63	14.4± 1.6	14.2±1.2
^{142}Ba	255.3	0.85 ±0.05	4.67±0.26	90	20.2± 1.6	1.29 ±0.03	5.73±0.46	22.5± 1.9	≈20
^{144}La	397.3					5.51 ±0.48	5.94±0.65	93 ±13	
^{148}Ce	291.8	1.00 ±0.25	2.15±0.43	68	68 ±22				
^{148}Pr	301.7	0.84 ±0.38	2.15±0.43	99	40 ±20	1.94 ±0.07	4.17±0.67	47 ± 8	90.9±0.4
^{153}Pm	127.3					0.228±0.007	1.29±0.08	17.7± 1.2	≈14

[a] Estimated fractional cumulative yield. See text for explanation.
[b] Data from Wilhelmy, Ref. 59.
[c] Recommend cumulative fission-product yield, Rider and Meek, Ref. 1.
[d] Branching ratio either evaluated or else the best recommended experimental value, *Table of Isotopes*, Ref. 27.

Northcutt of the ORNL Analytical Chemistry Division for careful preparation of the sample in the capsule and carrier, and for participation in the data taking following the 4-s irradiation. This research was sponsored by the USDOE Office of Energy Research, Division of Nuclear Physics, under Contract No. W-7405-eng-26 with Union Carbide Corporation.

[1]B. F. Rider and M. E. Meek, Report No. NEDO-12154-2(E) (General Electric Company, 1978).
[2]E. A. C. Crouch, At. Data Nucl. Data Tables 19, 419 (1977).
[3]E. K. Hyde, *The Nuclear Properties of the Heavy Elements* (Dover, New York, 1971), p. 112.
[4]H. N. Erten and N. K. Aras, J. Inorg. Nucl. Chem. 41, 149 (1979).
[5]R. M. Harbour and K. W. MacMurdo, J. Inorg. Nucl. Chem. 34, 2109 (1972).
[6]H. R. von Gunten, K. F. Flynn, and L. E. Glendenin, Phys. Rev. 161, 1192 (1967).
[7]A. Ramaswami, S. P. Dange, S. Prakash, and M. V. Ramaniah, J. Inorg. Nucl. Chem. 41, 1649 (1979).
[8]T. Datta, S. P. Dange, S. B. Manohar, A. G. C. Nair, S. Prakash, and M. V. Ramaniah, Phys. Rev. C 21, 1411 (1980).
[9]S. Singh, T. Datta, R. Trehan, P. P. Venkatesan, S. P. Dange, S. B. Manohar, A. G. C. Nair, S. Prakash, and M. V. Ramaniah, in *Proceedings of the Nuclear Physics and Solid State Physics Symposium, Pune, 1977* (INSDOC, New Delhi, 1978), Vol. 20B, p. 249.
[10]D. E. Troutner and R. M. Harbour, Phys. Rev. C 4, 505 (1971).
[11]R. M. Harbour, D. E. Troutner, and K. W. MacMurdo, Phys. Rev. C 10, 769 (1974).
[12]J. K. Dickens and J. W. McConnell, Nucl. Sci. Eng. 73, 42 (1980).
[13]J. K. Dickens, J. F. Emery, T. A. Love, J. W. McConnell, K. J. Northcutt, R. W. Peelle, and H. Weaver, Oak Ridge National Laboratory Report No. NUREG/CR-0194, ORNL/NUREG-34, 1978.
[14]J. K. Dickens, J. F. Emery, T. A. Love, J. W. McConnell, K. J. Northcutt, R. W. Peelle, and H. Weaver, Oak Ridge National Laboratory Report No. ORNL/NUREG-14, 1977.
[15]C. M. Davisson and R. D. Evans, Rev. Mod. Phys. 24, 79 (1952); C. M. Davisson, in *Beta- and Gamma-Ray Spectroscopy*, edited K. Siegbahn (Interscience, New York, 1955), pp. 24 and 857.
[16]J. K. Dickens, J. F. Emery, T. A. Love, J. W. McConnell, K. J. Northcutt, R. W. Peelle, and H. Weaver, Oak Ridge National Laboratory Report No. NUREG/CR-0171, ORNL/NUREG-47, 1978.
[17]K. J. Northcutt and J. F. Emery (private communication).
[18]J. K. Dickens, Nucl. Sci. Eng. 70, 177 (1979).
[19]A. Okazaki, W. H. Walker, and C. B. Bigham, Can. J. Phys. 44, 237 (1966).
[20]R. C. Hawkings, W. J. Edwards, and W. J. Olmstead, Can. J. Phys. 49, 785 (1971).
[21]H. Thierens, D. de Frenne, E. Jacobs, A. de Clercq, P. D'hondt, and A. J. Deruytter, Nucl. Instrum. Methods 134, 299 (1976).
[22]A. C. Wahl, R. L. Ferguson, D. R. Nethaway, D. E. Troutner, and K. Wolfsberg, Phys. Rev. 126, 1112 (1962).
[23]J. K. Dickens, Radiochem. Radioanal. Lett. 39, 107 (1979).
[24]M. C. Thompson, M. L. Hyder, and R. J. Reuland, J. Inorg. Nucl. Chem. 33, 1553 (1971).
[25]R. W. Benjamin, Savannah River Laboratory Report No. DP-MS-75-87, 1975.
[26]H. G. Borner, W. F. Davidson, J. Almeida, J. Blachot, J. A. Pinston, and P. H. M. Van Assche, Nucl. Instum. Methods 164, 579 (1979).
[27]*Table of Isotopes*, edited by C. M. Lederer and V. S. Shirley, seventh edition (Wiley, New York, 1978).
[28]R. K. Smither, E. Bieber, T. vonEgidy, W. Kaiser, and K. Wien, Phys. Rev. 187, 1632 (1969).
[29]L. A. Kroger and C. W. Reich, Nucl. Data Sheets 10, 429 (1973).
[30]H. H. Hansen, E. Celen, G. Grosse, D. Mouchel, A. Nylandsted Larsen, and R. Vaninbroukx, Z. Phys. A 290, 113 (1979).
[31]G. Franz and G. Herrmann, J. Inorg. Nucl. Chem. 40, 945 (1978).
[32]E. W. Schneider, M. D. Glascock, W. B. Walters, and R. A. Meyer, Z. Phys. A 291, 77 (1979).
[33]T. Bjornstad, E. Kvale, G. Skarnemark, and P. O. Aronsson, J. Inorg. Nucl. Chem. 39, 1929 (1977).
[34]Z. Matumoto and T. Tamura, J. Phys. Soc. Jpn. 29, 1116 (1970).
[35]P. Fettweis and P. del Marmol, Z. Phys. A 275, 359 (1975).
[36]B. Harmatz, Nucl. Data Sheets 27, 453 (1979).
[37]H. Niizeki, S. Kageyama, T. Tamura, and Z. Matumoto, J. Phys. Soc. Jpn. 47, 26 (1979).
[38]G. Skarnemark, P. O. Aronsson, T. Bjornstad, and E. Kvale, J. Inorg. Nucl. Chem. 39, 1487 (1977).
[39]D. de Frenne, H. Thierens, E. Jacobs, P. de Gelder, P. D'hondt, A. de Clercq, K. Heyde, and A. J. Deruytter, Phys. Rev. C 18, 486 (1978).
[40]J. Blachot and C. Fiche, At. Data Nucl. Data Tables 20, 241 (1977).
[41]H. J. Kim, Nucl. Data Sheets 16, 107 (1975).
[42]M. A. Lee and W. L. Talbert, Jr., Phys. Rev. C 21, 328 (1980).
[43]Y. Ikeda, H. Yamamoto, K. Kawade, T. Takeuchi, T. Katoh, and T. Nagahara, J. Phys. Soc. Jpn. 47, 1039 (1979).
[44]K. Summerer, N. Kaffrell, E. Stender, N. Troutmann, K. Broden, G. Skarnemark, and J. A. Maruhn, Nucl. Phys. A339, 74 (1980).
[45]H. Thierens, D. de Frenne, E. Jacobs, A. de Clercq, P. D'hondt, and A. J. Deruytter, Phys. Rev. C 14, 1058 (1976).
[46]D. de Frenne, H. Thierens, E. Jacobs, P. de Gelder, A. de Clercq, P. D'hondt, and A. J. Deruytter, Phys. Rev. C 21, 629 (1980).
[47]D. R. Nethaway, A. L. Prindle, W. A. Myers, W. C. Fuqua, and M. V. Kantelo, Phys. Rev. C 16, 1907 (1977).
[48]S. Nagy, K. F. Flynn, J. E. Gindler, J. W. Meadows,

and L. E. Glendenin, Phys. Rev. C 17, 163 (1978).
[49]D. R. Nethaway, University of California at Berkeley Report No. UCRL-51538, 1974.
[50]R. H. Goechermann and I. Perlman, Phys. Rev. 76, 628 (1949).
[51]A. H. Jaffey and J. L. Lerner, Nucl. Phys. A145, 1 (1970).
[52]A. C. Wahl, A. E. Norris, R. A. Rouse, and J. C. Williams, in *Proceedings of the Second International Atomic Energy Symposium on the Physics and Chemistry of Fission, Vienna, 1969* (IAEA, Vienna, 1969), p. 813.
[53]J. Gindler, Phys. Rev. C 19, 1806 (1979).
[54]J. G. Cuninghame, Report No. IAEA-213, Vol. I, 1978; U. K. Atomic Energy Research Establishment, Harwell, Report No. AERE-R8753, 1977.
[55]P. O. Strom, D. L. Love, A. E. Greendale, A. A. Delucchi, D. Sam, and N. E. Ballou, Phys. Rev. 144, 984 (1966).
[56]F. G. Perey, Oak Ridge National Laboratory Report No. ORNL/TM-6267, ENDF-259, 1978, p. 26.
[57]B. W. Arden and K. N. Astill, *Numerical Algorithms: Origins and Applications* (Addison-Wesley, Reading, Mass. 1970), p. 168.
[58]M. D. Goldberg, S. F. Mughabghab, S. N. Purohit, B. A. Magurno, and V. M. May, Brookhaven National Laboratory Report No. BNL-325, second ed., Suppl. No. 2, 1966.
[59]J. B. Wilhelmy, University of California at Berkeley, Report No. UCRL-18978, 1969.